1969

LIBRARY AND
DOCUMENTS SECTION

UCRL-18630

Cy. 2

OFF-ENERGY-SHELL BEHAVIOR OF PARTIAL-WAVE SCATTERING AMPLITUDES

Thomas R. Mongan

November 26, 1968

TWO-WEEK LOAN COPY

This is a Library Circulating Copy which may be borrowed for two weeks. For a personal retention copy, call Tech. Info. Division, Ext. 5545

T

LAWRENCE RADIATION LABORATORY
UNIVERSITY of CALIFORNIA BERKELEY

UCRL-18630

DISCLAIMER

This document was prepared as an account of work sponsored by the United States Government. While this document is believed to contain correct information, neither the United States Government nor any agency thereof, nor the Regents of the University of California, nor any of their employees, makes any warranty, express or implied, or assumes any legal responsibility for the accuracy, completeness, or usefulness of any information, apparatus, product, or process disclosed, or represents that its use would not infringe privately owned rights. Reference herein to any specific commercial product, process, or service by its trade name, trademark, manufacturer, or otherwise, does not necessarily constitute or imply its endorsement, recommendation, or favoring by the United States Government or any agency thereof, or the Regents of the University of California. The views and opinions of authors expressed herein do not necessarily state or reflect those of the United States Government or any agency thereof or the Regents of the University of California.

Submitted to Phys. Rev.

UCRL-18630
Preprint

UNIVERSITY OF CALIFORNIA

Lawrence Radiation Laboratory
Berkeley, California

AEC Contract No. W-7405-eng-48

OFF-ENERGY-SHELL BEHAVIOR OF PARTIAL-WAVE SCATTERING AMPLITUDES

Thomas R. Mongan

November 26, 1968

UCRL-18630

OFF-ENERGY-SHELL BEHAVIOR OF PARTIAL-WAVE SCATTERING AMPLITUDES*

Thomas R. Mongan

Lawrence Radiation Laboratory
University of California
Berkeley, California

November 26, 1968

ABSTRACT

We compare the off-energy-shell behavior of several potential models for the nucleon-nucleon interaction. This is done by comparing the Kowalski-Noyes half-off-shell functions $f_\ell(p,k)$ resulting from the different models.

I. INTRODUCTION

We have presented several separable potential models of the nucleon-nucleon interaction and claimed that these models will be useful in probing the off-energy-shell behavior of the nucleon-nucleon scattering amplitude.[1,2] Therefore, it seems useful to display the off-energy-shell behavior of our models and compare this off-shell behavior with the off-shell behavior produced by some other potential models of the nucleon-nucleon interaction.

The point of the present paper is that the off-energy-shell behavior of separable potential models is <u>not</u> qualitatively different from the off-shell behavior produced by local soft-core Yukawa potential models. Thus, separable potential models lead to off-energy-shell scattering amplitudes that are as close to physical reality as the amplitudes resulting from these local potential models. Therefore, at the present state of our knowledge of the nucleon-nucleon interaction, the use of separable potential models in calculations involving off-energy-shell nucleon-nucleon scattering amplitudes is strongly indicated, because of the great convenience and simplicity of the separable potential models.

If the half-off-energy-shell partial-wave scattering amplitude $T_\ell(p,k;\, k^2)$ goes to zero as $k^2 \to \infty$, which is true in potential theory, the half-off-shell amplitude is determined by the scattering region $(k^2 > 0)$ values of the on-shell amplitude and the Kowalski-Noyes[3,4] half-off-shell function $f_\ell(p,k)$, where $f_\ell(p,k)$ is a <u>real</u> function.

Similarly, it can be shown that the full off-shell amplitude $T_\ell(p,p';\, k^2)$ is determined for all values of k^2 by the scattering region $(k^2 > 0)$ values of the on-shell amplitude and the half-off-shell function $f_\ell(p,k)$, if $T_\ell(p,p';\, k^2) \to 0$ as $k^2 \to \infty$.[5] Consequently, in this paper we compare the off-energy-shell behavior of several types of potential models of the nucleon-nucleon interaction by displaying the half-off-shell functions $f_\ell(p,k)$ for $k^2 > 0$, generated by the various models.

II. EQUATIONS AND CONVENTIONS

The half-off-shell partial-wave nucleon-nucleon scattering amplitude $T_\ell(p,k;k^2)$ is determined in potential theory by the two-particle nonrelativistic Lippmann-Schwinger equation

$$T_\ell(p,k;\, k^2) = V_\ell(p,k) + \frac{2\mu}{\hbar^2} \int_0^\infty \frac{q^2\, dq\, V_\ell(p,q)\, T_\ell(q,k;\, k^2)}{k^2 - q^2 + i\epsilon} , \qquad (1)$$

where the c.m. kinetic energy $E = \hbar^2 k^2/2\mu$ and μ is the reduced mass of the two nucleons.

It can be shown[6] on the basis of time reversal and unitarity alone that the half-off-shell amplitude $T_\ell(p,k;\, k^2)$ can be written

$$T_\ell(p,k;\, k^2) = f_\ell(p,k)\, T_\ell(k^2),$$

where $f_\ell(p,k)$ is a <u>real</u> function and $T_\ell(k^2)$ is the on-shell partial-wave scattering amplitude

$$T_\ell(k^2) = -\frac{\hbar^2}{\pi\mu k}\, e^{i\delta_\ell(k^2)} \sin \delta_\ell(k^2) .$$

In fact, by performing a Fredholm reduction on the singular integral Eq. (1), we can show[3] that the half-off-shell function $f_\ell(p,k)$ is determined in potential theory by the nonsingular integral equation

$$f_\ell(p,k) = \frac{V_\ell(p,k)}{V_\ell(k,k)} + \frac{2\mu}{h^2}\int_0^\infty \frac{q^2 dq}{k^2 - q^2}\left[V_\ell(p,q) - \frac{V_\ell(p,k)\, V_\ell(k,q)}{V_\ell(k,k)}\right] \times f_\ell(q,k) \quad . \tag{2}$$

The real function $f_\ell(p,k)$ has the threshold behavior $f_\ell(p,k) \sim p^\ell$ as $p \to 0$ and $f_\ell(p,k) \sim k^{-\ell}$ as $k \to 0$. Of course, $f_\ell(k,k) \equiv 1$ and $f_\ell(p,k) \to \infty$ when $T_\ell(k^2) \to 0$.

In the separable potential models we presented earlier, the potential in uncoupled partial waves is

$$V_\ell(p,p') = g_\ell(p)\, g_\ell(p') - h_\ell(p)\, h_\ell(p') \quad ;$$

and the half-off-shell function can be written

$$f_\ell(p,k) = N_\ell(p,k)/N_\ell(k,k) \quad , \tag{3}$$

where

$$N_\ell(p,k) = g_\ell(p)\, g_\ell(k)\left[1 + \frac{2\mu}{\hbar^2} P\int_0^\infty \frac{dq\, q^2\, h_\ell^2(q)}{k^2 - q^2}\right]$$

$$- h_\ell(p)\, h_\ell(k)\left[1 - \frac{2\mu}{\hbar^2} P\int_0^\infty \frac{dq\, q^2}{k^2 - q^2}\, g_\ell^2(q)\right]$$

$$- \left[g_\ell(p)\, h_\ell(k) + h_\ell(p)\, g_\ell(k)\right] \frac{2\mu}{\hbar^2} P\int_0^\infty \frac{dq\, q2}{k^2 - q^2}\, g_\ell(q)\, h_\ell(q) \quad ,$$

and P indicates a principal value integral. For a single-term separable potential, we have $V_\ell(p,p') = \lambda\, g_\ell(p)\, g_\ell(p')$ with $\lambda = \pm 1$

and the half-off-shell function is

$$f_\ell(p,k) = g_\ell(p)/g_\ell(k) \quad . \tag{4}$$

We have compared the half-off-shell functions in the uncoupled partial waves $^1S_0$, $^1P_1$, and $^1D_2$ resulting from four different separable potential models of the general form

$$V_\ell(p,p') = g_\ell(p)\, g_\ell(p') - h_\ell(p)\, h_\ell(p') \quad ,$$

and from three different local soft-core Yukawa potential models of the nucleon-nucleon interaction. These potentials are:

(i) separable potential Case I of Ref. 2 with

$$g_\ell(p) = G_R\, p^\ell/(p^2 + a_R^2)^{(\ell+1)/2} \quad ;$$

$$h_\ell(p) = G_A\, p^\ell/(p^2 + a_A^2)^{(\ell+1)/2} \quad .$$

The potential parameters in the different partial waves are given in Table I;

(ii) separable potential Case II of Ref. 2 with

$$g_\ell(p) = G_R p^\ell/(p^2 + a_R^2)^{(\ell+2)/2} \quad ;$$

$$h_\ell(p) = G_A p^\ell/(p^2 + a_A^2)^{(\ell+2)/2} \quad .$$

The potential parameters for the different partial waves are displayed in Table I;

(iii) separable potential Case III of Ref. 2 with

$$g_\ell(p) = \frac{G_R\, p^2}{\left(p^2 + \frac{\mu_R^2}{4}\right)} \left[\frac{1}{\pi p^2}\, Q_\ell\left(1 + \frac{\mu_R^2}{2p^2}\right)\right]^{\frac{1}{2}} ;$$

$$h_\ell(p) = G_A \left[\frac{1}{\pi p^2}\, Q_\ell\left(1 + \frac{\mu_A^2}{2p^2}\right)\right]^{\frac{1}{2}} ,$$

where $Q_\ell(x)$ is the Legendre function of the second kind and the potential parameters are again given in Table I;

(iv) separable potential Case IV of Ref. 2 with

$$g_\ell(p) = G_R\, p^\ell/(p^2 + a_R^2)^{(\ell+1)} ;$$

$$h_\ell(p) = G_A\, p^\ell/(p^2 + a_A^2)^{(\ell+1)} .$$

Note that (iv) is identical to (ii) in the partial wave $^1S_0$. The potential parameters in the different partial waves are entered in Table I;

(v) the local soft-core potential models of Reid.[17] In the partial wave $^1S_0$, the potentials are

$$V_A(x) = -h\frac{e^{-x}}{x} - 1650.6\,\frac{e^{-4x}}{x} + 6484.2\,\frac{e^{-7x}}{x}$$

and

$$V_B(x) = -h\frac{e^{-x}}{x} + 105.32\,\frac{e^{-3x}}{x} - 2401.9\,\frac{e^{-4x}}{x} + 5598.2\,\frac{e^{-6x}}{x} .$$

In the partial wave $^1P_1$, the potentials are

$$V_A(x) = 3h \frac{e^{-x}}{x} - 634.39 \frac{e^{-2x}}{x} + 2163.4 \frac{e^{-3x}}{x}$$

or

$$V_B(x) = 3h \frac{e^{-x}}{x} - 240 \frac{e^{-2x}}{x} + 17000 \frac{e^{-6x}}{x} .$$

Finally, in the partial $^1D_2$, the potentials are

$$V_A(x) = - h \frac{e^{-x}}{x} - 318.64 \frac{e^{-3x}}{x} + 526.27 \frac{e^{-5x}}{x}$$

or

$$V_B(x) = -h \frac{e^{-x}}{x} - 12.322 \frac{e^{-2x}}{x} - 1112.6 \frac{e^{-4x}}{x} + 6484.2 \frac{e^{-7x}}{x} .$$

In all these potentials $h = 10.463$ MeV and $x = \mu r$ with $\mu = 0.7\ F^{-1}$;

(vi) the local soft-core potential model of Ulehla, Bystricky, and Lehar.[8] In the partial wave $^1S_0$, this potential is

$$V(x) = \frac{m_\pi^2}{m_N}\left(-2.06 \frac{e^{-x}}{x} + 31.8 \frac{e^{-2x}}{x} - 179.6 \frac{e^{-3x}}{x} + 212.2 \frac{e^{-4x}}{x}\right) ,$$

while in $^1P_1$, the potential is

$$V(x) = \frac{m_\pi^2}{m_N}\left(-1.31 \frac{e^{-x}}{x} + 12.25 \frac{e^{-2x}}{x}\right)$$

and in $^1D_2$, the potential is

$$V(x) = \frac{m_\pi^2}{m_N}\left(-0.962 \frac{e^{-x}}{x} + 2.4 \frac{e^{-2x}}{x} - 0.2 \frac{e^{-3x}}{x} - 39.2 \frac{e^{-4x}}{x}\right) ,$$

where $m_\pi = 139.51$ MeV, $m_N = 937.0$ MeV and $x = \mu r$ with $\mu = 0.707\ F^{-1}$.

In momentum space, the potentials of Reid and Ulehla et al. are given by

$$V_\ell(p,q) = \sum_{i=1}^{4} \frac{G_i}{\pi pq} Q_\ell\left(\frac{p^2 + q^2 + \mu_i^2}{2pq}\right) ,$$

where $Q_\ell(x)$ is the Legendre function of the second kind. The coupling strength G_i and the inverse ranges μ_i in the three cases are given in Table II.

Additionally, in the partial wave $^1S_0$, we consider Tabakin's[9] single term separable potential model of the $^1S_0$ interaction. In Tabakin's model

$$V_\ell(p,p') = g_\ell(p)\, g_\ell(p') , \tag{5}$$

with

$$g_\ell(p) = \alpha(k_c^2 - p^2)\left(\frac{p^2 + d^2}{p^2 + b^2}\right) \frac{1}{p^4 + a^4} ,$$

where $\alpha^2 = 400.8434\ F^{-3}$, $k_c = 1.7\ F^{-1}$, $a = 4.05\ F^{-1}$, $b = 1.08548\ F^{-1}$, and $d = 1.683\ F^{-1}$.

III. CALCULATIONS AND RESULTS

First we check the on-shell properties of the different potential models. In Tables III through V, we present the values of the phase shifts generated by the different potential models at selected values of the laboratory kinetic energy.

Next, we obtain the half-off-shell functions $f_\ell(p,k)$ resulting from our separable potential models from Eq. (3) and we display $f_\ell(p,k)$ vs p for fixed values of the laboratory kinetic energy $E_{LAB} = 2(\hbar^2 k^2/2\mu)$ in Figs. 1 through 8. Note that in the partial wave $^1S_0$ the Case II and Case IV potentials are identical and the Case III potential of Ref. 2 has an off-shell behavior substantially different from the other separable potential models. This behavior is also characteristic of the Case I and Case II fits of Ref. 1, which have specially modified repulsive form factors. The different behavior of $f_\ell(p,k)$ for large p in the various separable potential models is clearly displayed in Figs. 5 through 8.

We now compare the off-shell behavior of our separable potential models of the nucleon-nucleon interaction with the Reid and Ulehla et al. local potential models and Tabakin's separable $^1S_0$ potential. We shall choose Case II of Ref. 2 to represent our separable potential models in this comparison, because it gives the best fit to the on-shell data.

For the local potential models, $f_\ell(p,k)$ is obtained by solving the integral equation (2) numerically as a matrix inversion problem.

For the Case II of Ref. 2 separable potential model, $f_\ell(p,k)$ is obtained from Eq. (3), while Eq. (4) yields $f_\ell(p,k)$ for the Tabakin model. We display the results as curves of $f_\ell(p,k)$ vs p at fixed values of k, in Figs. 9 through 16.

When we compare the off-shell behavior resulting from the local Yukawa potential models with the separable potential models represented by Case II of Ref. 2, we find that the off-shell functions in partial waves with $\ell = 1$ and $\ell = 2$ are quite similar, especially at high energy (i.e., a laboratory kinetic energy of 300 MeV). The agreement would be even better if we had chosen Case IV of Ref. 2 to represent our separable potential models, because the Case IV potentials lead to an asymptotic behavior

$$f_\ell(p,k) \sim 1/p^{(\ell+2)} \quad \text{as} \quad p \to \infty \quad ,$$

which is the same as the asymptotic behavior resulting from a superposition of Yukawa potentials. Correspondingly, the agreement of the off-shell functions resulting from the local Yukawa models with the off-shell functions generated by the separable model is somewhat worse in Cases I and III.

The greatest difference between the off-shell functions resulting from the local potentials and our separable potential models is in the partial wave $^1S_0$ at laboratory kinetic energy of 400 MeV and momentum $p = 0$, where $f_\ell(p,k) \approx 0$ for the local potential models and $f_\ell(p,k)$ is of order 1 for the separable models.

Also, in the partial wave $^1S_0$, the function $f_\ell(p,k)$ produced by our separable potential models falls off more slowly as $p \to \infty$ than the off-shell functions resulting from the local potential models. Notice that the single separable potential model of the $^1S_0$ interaction given by Tabakin seems to lead to an off-shell function somewhat different from those produced by other models.

Our contention that the off-energy-shell behavior of separable potential models is not in contradiction with experiment and is not drastically different in a calculational sense from the off-shell behavior produced by local potentials is borne out, respectively, by the success of Tabakin's earlier separable potential model of the nucleon-nucleon interaction in nuclear physics calculations[10] and by the agreement of the separable potential p-p Bremsstrahlung calculation of Pearce, Gale, and Duck,[11] with the local potential calculations and with experiment.

Our results have been checked by utilizing programs which solve the Lippmann-Schwinger Eq. (1) as a complex matrix inversion problem to obtain the amplitudes $T_\ell(p,k;\, k^2)$ and $T_\ell(k^2)$. These amplitudes determine $f_\ell(p,k)$ by the equation $f_\ell(p,k) = T_\ell(p,k,k^2)/T_\ell(k^2)$, and this result is checked against $f_\ell(p,k)$ calculated from Eqs. (2) and (3).

IV. COMMENTS AND CONCLUSIONS

We would first like to remark on Tabakin's[9] single separable potential model of the $^1S_0$ nucleon-nucleon interaction as set forth in Eq. (5). This model leads to a pole in the full off-energy-shell amplitude $T_\ell(p,k;\, k^2)$ at $k^2 = k_c^{\,2}$ which does not occur in the actual full off-shell amplitude.[5] If the Tabakin model is used in three-body scattering calculations, this spurious singularity or "positive energy bound state," as Tabakin calls it, will lead to cuts in the three-body scattering amplitudes similar to those resulting from the scattering of a free particle off a real physical bound state of the other two.[12] It is difficult to predict the effects or assess the physical significance of these somewhat artificial cuts. Although the Tabakin potential yields an off-shell function $f_\ell(p,k)$ that is rather different from the off-shell functions resulting from our separable potential models or from the local soft-core Yukawa potential models, we believe that the Tabakin potential may provide a useful model for the off-shell function $f_\ell(p,k)$. If the Tabakin model is used only to generate the off-shell function $f_\ell(p,k)$, the half-off-shell scattering amplitude may be written $T_\ell(p,k;\, k^2) = \alpha_\ell(p)\, \beta_\ell(k)\, T_\ell(k^2)$ with $T_\ell(k^2)$ written in terms of the experimental phase shifts, and $\alpha_\ell(p)$ and $\beta_\ell(k)$ obtained directly from the Tabakin model. Additionally, a separable model of the off-shell factor $f_\ell(p,k)$ in the form $f_\ell(p,k) = \alpha_\ell(p)\, \beta_\ell(k)$ is very useful when studying the full off-shell amplitude.[5]

It seems that the necessity of fitting the on-shell data constrains our separable potential models and the local soft-core

Yukawa potentials to share the same qualitative off-shell behavior. This is not surprising in view of the smoothness of the mathematical forms of these potentials.

Our separable potential models do show some variation in off-shell behavior, especially for large values of p in $f_\ell(p,k)$. This reinforces our hopes that the use, in calculations involving the off-energy-shell two-body scattering amplitude, of the form

$$T_\ell(p,p';\, k^2) = F_\ell(p,p';\, k^2)\; T_\ell(k^2) \quad ,$$

with $F_\ell(p,p';\, k^2)$ determined by the separable potential models and $T_\ell(k^2)$ written in terms of the experimental phase shifts, will enable us to discern the sensitivity of these calculations to the off-energy-shell behavior of the amplitudes.

We have demonstrated that separable potential models lead to an off-energy-shell behavior, which is <u>not</u> qualitatively different from the off-shell behavior resulting from local soft-core Yukawa potential models of the nucleon-nucleon interaction. Since separable potential models do not produce any freakish effects off the energy shell, they seem to have an equally valid claim to presenting a realistic representation of the off-shell nucleon-nucleon interaction as the local potential models. Therefore, since the separable potential models are so much simpler, their use in calculations involving the off-energy-shell nucleon-nucleon partial-wave scattering amplitude is strongly indicated.

FOOTNOTES AND REFERENCES

* This work was supported in part by the U.S. Atomic Energy Commission.

1. Thomas R. Mongan, Phys. Rev. 175, (1968). We will call this Ref. 1.
2. Thomas R. Mongan, Lawrence Radiation Laboratory Report UCRL-18501, October 1968. We will call this Ref. 2.
3. K. L. Kowalski, Phys. Rev. Letters 15, 798 (1965).
4. H. P. Noyes, Phys. Rev. Letters 15, 538 (1965).
5. T. R. Mongan, Lawrence Radiation Laboratory Report UCRL-17452, March 1967 (unpublished).
6. M. I. Sobel, Phys. Rev. 138, B1517 (1965).
7. Roderick V. Reid, Jr., Local Phenomenological Nucleon-Nucleon Potentials, Center for Theoretical Physics, Laboratory for Nuclear Science, Massachusetts Institute of Technology Report No. CTP-40, August 1968 (unpublished).
8. I. Ulehla, J. Bystricky, and F. Lehar, Proc. International Nuclear Physics Conference, Gatlinburg, Tennessee, 1966 , p. 687.
9. F. Tabakin, Phys. Rev. 174, 1208 (1968).
10. F. Tabakin, Ann. Phys. (N.Y.) 30, 51 (1964).
11. W. A Pearce, W. A. Gale, and I. M. Duck, Nucl. Phys. B3, 241 (1967).
12. C. Lovelace, Phys. Rev. 135, B1225 (1964).

Table I. Potential parameters for the separable potentials of Ref. 2.

Case I				
Partial Wave	G_R $(\text{MeV F})^{\frac{1}{2}}$	a_R (F^{-1})	G_A $(\text{MeV F})^{\frac{1}{2}}$	a_A (F^{-1})
$^1S_0$	52.45	2.331	41.36	1.855
$^1P_1$	49.83	1.138	46.16	1.103
$^1D_2$	0.0	-	4.817	1.418
Case II				
Partial Wave	G_R $(\text{MeV/F})^{\frac{1}{2}}$	a_R (F^{-1})	G_A $(\text{MeV/F})^{\frac{1}{2}}$	a_A (F^{-1})
$^1S_0$	302.0	6.157	27.33	1.786
$^1P_1$	40.88	1.410	30.21	1.258
$^1D_2$	0.0	-	21.09	1.944

Table I (Continued).

Case III

Partial Wave	G_R $(\text{MeV F})^{\frac{1}{2}}$	μ_R (F^{-1})	G_A $(\text{MeV F})^{\frac{1}{2}}$	μ_A (F^{-1})
$^1S_0$	20.84	2.225	10.00	1.300
$^1P_1$	26.53	0.644	31.53	1.256
$^1D_2$	0.0	-	10.61	1.415

Case IV

Partial Wave	G_R $[\text{MeV F}^{-(2\ell+1)}]^{\frac{1}{2}}$	a_R (F^{-1})	G_A $[\text{MeV F}^{-(2\ell+1)}]^{\frac{1}{2}}$	a_A (F^{-1})
$^1S_0$	302.0	6.157	27.33	1.786
$^1P_1$	121.6	1.967	49.73	1.566
$^1D_2$	0.0	-	530.5	2.721

Table II. Parameters of the soft-core local potentials of Reid and Ulehla et al.

$$V_\ell(p,q) = \sum_{i=1}^{4} \frac{G_i}{\pi pq} Q_\ell\left(\frac{p^2 + q^2 + \mu_i^2}{2pq}\right)$$ where the μ_i are in inverse Fermis (F^{-1}) and G_i are in MeV F.

Potential	$\mu_1(F^{-1})$	G_1(MeV F)	$\mu_2(F^{-1})$	G_2(MeV F)	$\mu_3(F^{-1})$	G_3(MeV F)	$\mu_4(F^{-1})$	G_4(MeV F)
Partial Wave $^1S_0$								
Reid A	0.7	-14.947	2.8	-2358.0	4.9	9263.1	-	0.0
Reid B	0.7	-14.947	2.1	150.46	2.8	-3431.3	4.2	7497.4
Ulehla et al.	0.707	-60.5	1.414	934.0	2.121	-5277.0	2.828	6234.0
Partial Wave $^1P_1$								
Reid A	0.7	31.389	1.4	-906.27	2.1	3090.6	-	0.0
Reid B	0.7	31.389	1.4	-342.9	4.2	24285.7	-	0.0
Ulehla et al.	0.707	-38.5	1.414	359.7	2.121	0.0	2.828	0.0

Table II (Continued).

Potential	$\mu_1(F^{-1})$	G_1(MeV F)	$\mu_2(F^{-1})$	G_2(MeV F)	$\mu_3(F^{-1})$	G_3(MeV F)	$\mu_4(F^{-1})$	G_4(MeV F)
Partial Wave $^1D_2$								
Reid A	0.7	-14.947	2.1	-455.20	3.5	751.81	-	0.0
Reid B	0.7	-14.947	1.4	-17.603	2.8	-1589.4	4.4	9263.1
Ulehla et al.	0.707	-28.3	1.414	71.0	2.121	5.9	2.828	-1150.0

Table III. $^1S_0$ phase shift in degrees generated by different potential models at selected values of the laboratory kinetic energy.

Potential Models	50 MeV	100 MeV	150 MeV	200 MeV	250 MeV	300 MeV	350 MeV
Mongan Case I	40.0	24.6	14.1	6.2	-0.11	-5.2	-9.6
Mongan Case II	40.4	25.0	14.4	6.4	-0.05	-5.4	-10.0
Mongan Case III	30.3	16.9	9.1	3.8	-0.06	-3.1	-5.5
Reid A	38.6	24.3	14.0	5.8	-1.1	-7.0	-12.2
Reid B	38.4	24.1	13.9	5.7	-1.0	-6.8	-11.9
Ulehla et al.	39.6	24.9	14.6	6.6	-0.09	-5.4	-10.1
Tabakin Single Separable	37.0	22.9	13.2	5.4	-1.3	-7.4	-13.0

Table IV. $^1P_1$ phase shift in degrees generated by different potential models at selected values of the laboratory kinetic energy.

Potential Model	50 MeV	100 MeV	150 MeV	200 MeV	250 MeV	300 MeV	350 MeV
Mongan Case I	-3.2	-11.6	-18.2	-23.3	-27.2	-30.3	-32.8
Mongan Case II	-2.7	-12.3	-19.7	-24.9	-28.3	-30.6	-32.0
Mongan Case III	-3.0	-13.0	-20.0	-24.7	-28.0	-30.3	-32.0
Mongan Case IV	-3.6	-12.3	-19.7	-25.3	-29.2	-31.8	-33.3
Reid A	-4.3	-11.5	-18.7	-25.2	-30.9	-35.9	-40.4
Reid B	-5.5	-11.3	-18.0	-24.6	-30.9	-36.9	-42.4
Ulehla et al.	-5.7	-12.3	-17.1	-20.5	-23.2	-25.4	-27.1

Table V. $^1D_2$ phase shift in degrees generated by different potential models at selected values of the laboratory kinetic energy.

Potential Models	50 MeV	100 MeV	150 MeV	200 MeV	250 MeV	300 MeV	350 MeV
Mongan Case I	1.1	3.3	5.5	7.1	8.4	9.2	9.9
Mongan Case II	0.9	3.1	5.4	7.2	8.5	9.3	9.8
Mongan Case III	1.4	3.5	5.4	6.9	8.2	9.1	9.9
Mongan Case IV	0.8	2.8	5.2	7.2	8.6	9.5	9.8
Reid A	1.7	3.6	5.3	6.8	8.0	9.0	9.8
Reid B	1.7	3.6	5.4	6.9	8.1	8.9	9.4
Ulehla et al.	2.0	3.5	5.2	7.1	9.1	11.3	13.4

FIGURE CAPTIONS

Fig. 1. Noyes-Kowalski half-off-shell functions $f_\ell(p,k)$ for the separable potential models of Ref. 2 in the partial wave $^1S_0$ at a laboratory kinetic energy of 0 MeV. The dashed curve represents the Case I fit. The solid curve marks the Case II and Case IV fits, which are identical in the partial wave $^1S_0$. The Case III fit is indicated by the dotted curve.

Fig. 2. Noyes-Kowalski half-off-shell functions $f_\ell(p,k)$ for the separable potential models of Ref. 2 in the partial wave $^1S_0$ at a laboratory kinetic energy of 230 MeV. Description of the curves is as for Fig. 1.

Fig. 3. Noyes-Kowalski half-off-shell functions $f_\ell(p,k)$ for the separable potential models of Ref. 2 in the partial wave $^1S_0$ at a laboratory kinetic energy of 270 MeV. Description of the curves is as for Fig. 1.

Fig. 4. Noyes-Kowalski half-off-shell functions $f_\ell(p,k)$ for the separable potential models of Ref. 2 in the partial wave $^1S_0$ at a laboratory kinetic energy of 400 MeV. Description of the curves is as for Fig. 1.

Fig. 5. Noyes-Kowalski half-off-shell functions $f_\ell(p,k)$ for the separable potential models of Ref. 2 in the partial wave $^1P_1$ at a laboratory kinetic energy of 100 MeV. The dashed curve represents the Case I fit, the solid curve marks the Case II fit, the dotted curve indicates the Case III fit, and the dot-dash curve denotes the Case IV fit.

Fig. 6. Noyes-Kowalski half-off-shell functions $f_\ell(p,k)$ for the separable potential models of Ref. 2 in the partial wave $^1P_1$ at a laboratory kinetic energy of 300 MeV. Description of the curves is as for Fig. 5.

Fig. 7. Noyes-Kowalski half-off-shell functions $f_\ell(p,k)$ for the separable potential models of Ref. 2 in the partial wave $^1D_2$ at a laboratory kinetic energy of 100 MeV. Description of the curves is as for Fig. 5.

Fig. 8. Noyes-Kowalski half-off-shell functions $f_\ell(p,k)$ for the separable potential models of Ref. 2 in the partial wave $^1D_2$ at a laboratory kinetic energy of 300 MeV. Description of the curves is as for Fig. 5.

Fig. 9. Comparison of the Noyes-Kowalski half-off-shell functions $f_\ell(p,k)$ resulting from local potential models and separable potential models in the partial wave $^1S_0$ at a laboratory kinetic energy of 0 MeV. The solid curve denotes $f_\ell(p,k)$ resulting from the separable potential Case II of Ref. 2, which has been chosen as representative of the separable potential models of Ref. 2. The solid curve marked with Δ represents $f_\ell(p,k)$ resulting from Tabakin's single term separable potential model of the $^1S_0$ interaction. The dotted curve displays $f_\ell(p,k)$ produced by the local potential model of Ulehla et al. The dashed curve indicates $f_\ell(p,k)$ generated by the local potential model of Reid which we have called A in the text. The dot-dash curve signifies $f_\ell(p,k)$

resulting from the local potential model of Reid which we have called B in the text.

Fig. 10. Comparison of the Noyes-Kowalski half-off-shell functions $f_\ell(p,k)$ resulting from local potential models and separable potential models in the partial wave $^1S_0$ at a laboratory kinetic energy of 230 MeV. Description of the curves is as for Fig. 9.

Fig. 11. Comparison of the Noyes-Kowalski half-off-shell functions $f_\ell(p,k)$ resulting from local potential models and separable potential models in the partial wave $^1S_0$ at a laboratory kinetic energy of 270 MeV. Description of the curves is as for Fig. 9.

Fig. 12. Comparison of the Noyes-Kowalski half-off-shell functions $f_\ell(p,k)$ resulting from local potential models and separable potential models in the partial wave $^1S_0$ at a laboratory kinetic energy of 400 MeV. Description of the curves is as for Fig. 9.

Fig. 13. Comparison of the Noyes-Kowalski half-off-shell functions $f_\ell(p,k)$ resulting from local potential models and separable potential models in the partial wave $^1P_1$ at a laboratory kinetic energy of 100 MeV. The solid curve denotes $f_\ell(p,k)$ resulting from the separable potential Case II of Ref. 2, which has been chosen as representative of the separable potential models of Ref. 2. The dotted curve displays $f_\ell(p,k)$ producted by the local potential model of Ulehla et al.

The dashed curve indicates $f_\ell(p,k)$ generated by the local potential model of Reid which we have called A in the text. The dot-dash curve signifies $f_\ell(p,k)$ resulting from the local potential model of Reid which we have called B in the text.

Fig. 14. Comparison of the Noyes-Kowalski half-off-shell functions $f_\ell(p,k)$ resulting from local potential models and separable potential models in the partial wave $^1P_1$ at a laboratory kinetic energy of 300 MeV. Description of the curves is as for Fig. 13.

Fig. 15. Comparison of the Noyes-Kowalski half-off-shell functions $f_\ell(p,k)$ resulting from local potential models and separable potential models in the partial wave $^1D_2$ at a laboratory kinetic energy of 100 MeV. Description of the curves is as for Fig. 13.

Fig. 16. Comparison of the Noyes-Kowalski half-off-shell functions $f_\ell(p,k)$ resulting from local potential models and separable potential models in the partial wave $^1D_2$ at a laboratory kinetic energy of 300 MeV. Description of the curves is as for Fig. 13.

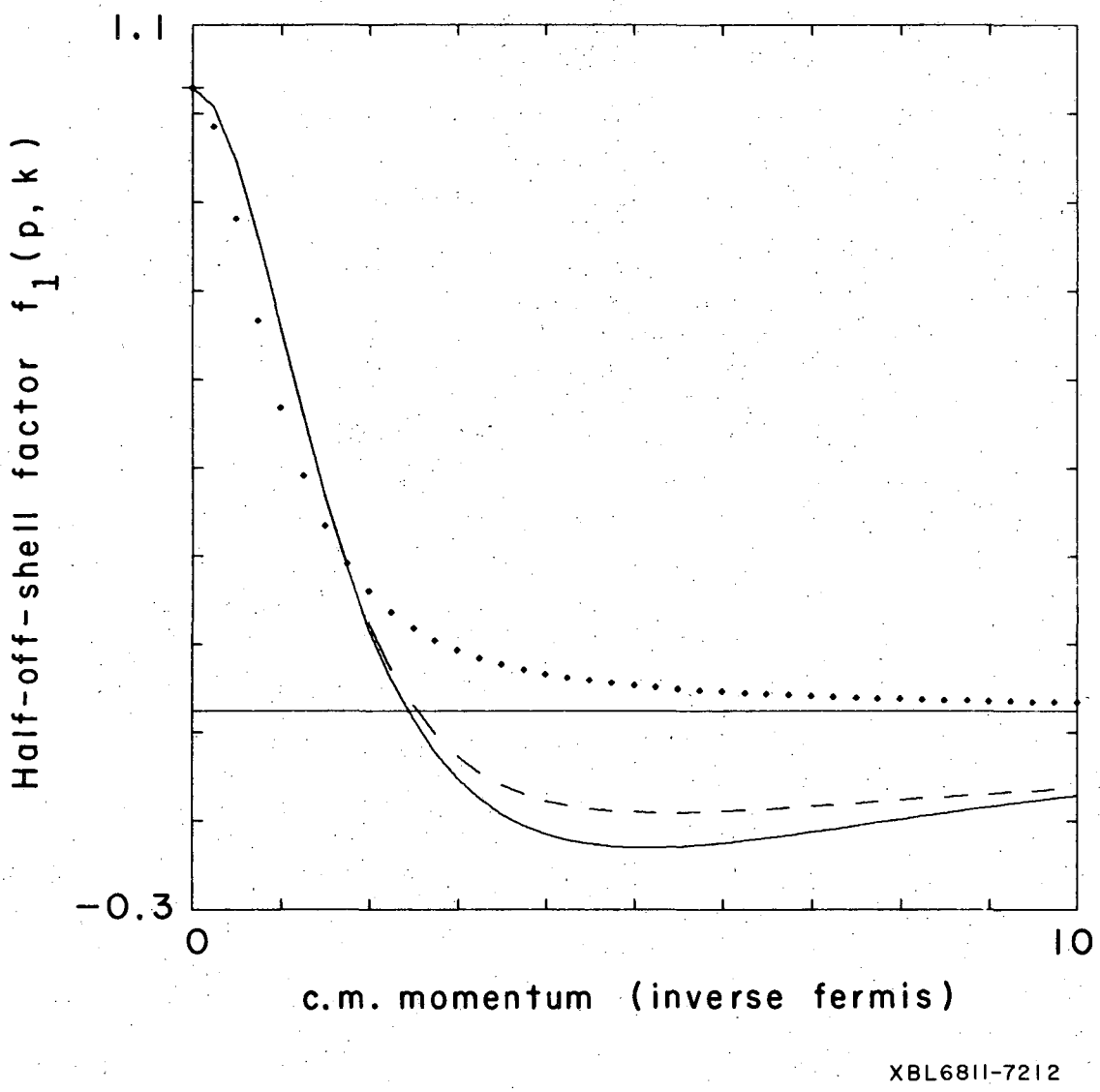
1.1
-0.3
0
10
Half-off-shell factor $f_1(p, k)$
c.m. momentum (inverse fermis)
XBL6811-7212

Fig. 1

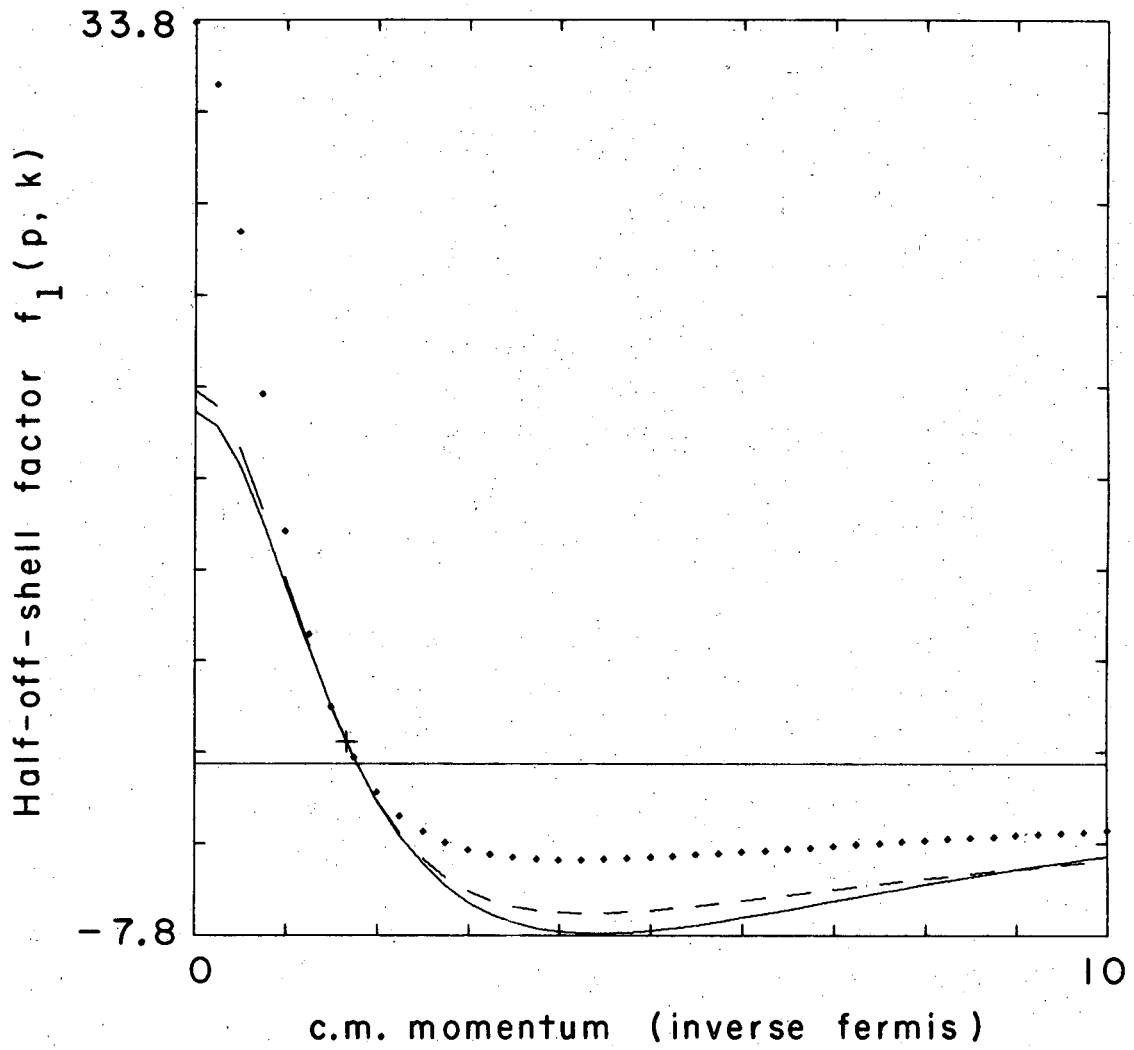

XBL6811-7213

Fig. 2

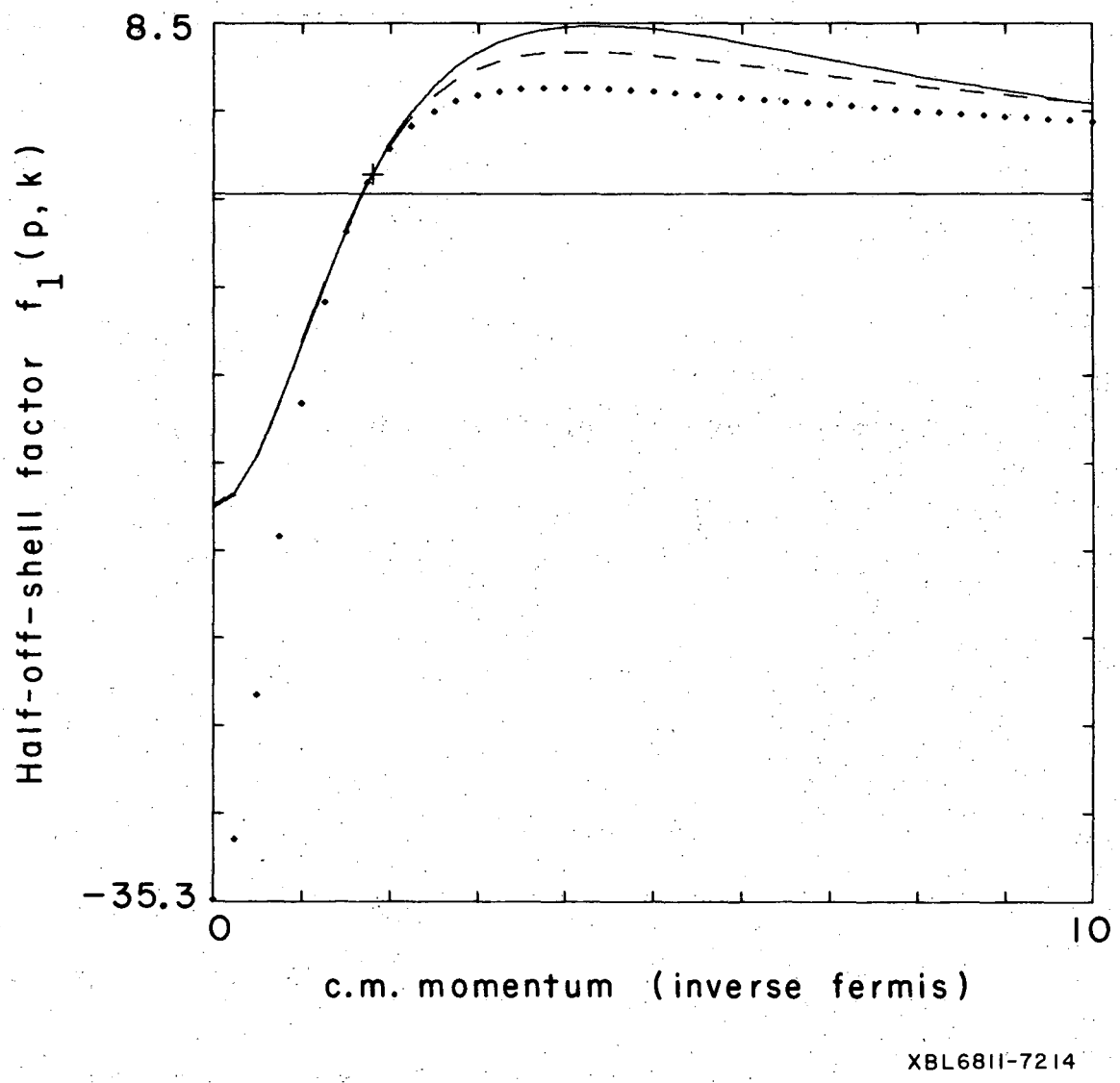
8.5
-35.3
0
10
Half-off-shell factor $f_1(p,k)$
c.m. momentum (inverse fermis)
XBL6811-7214

Fig. 3

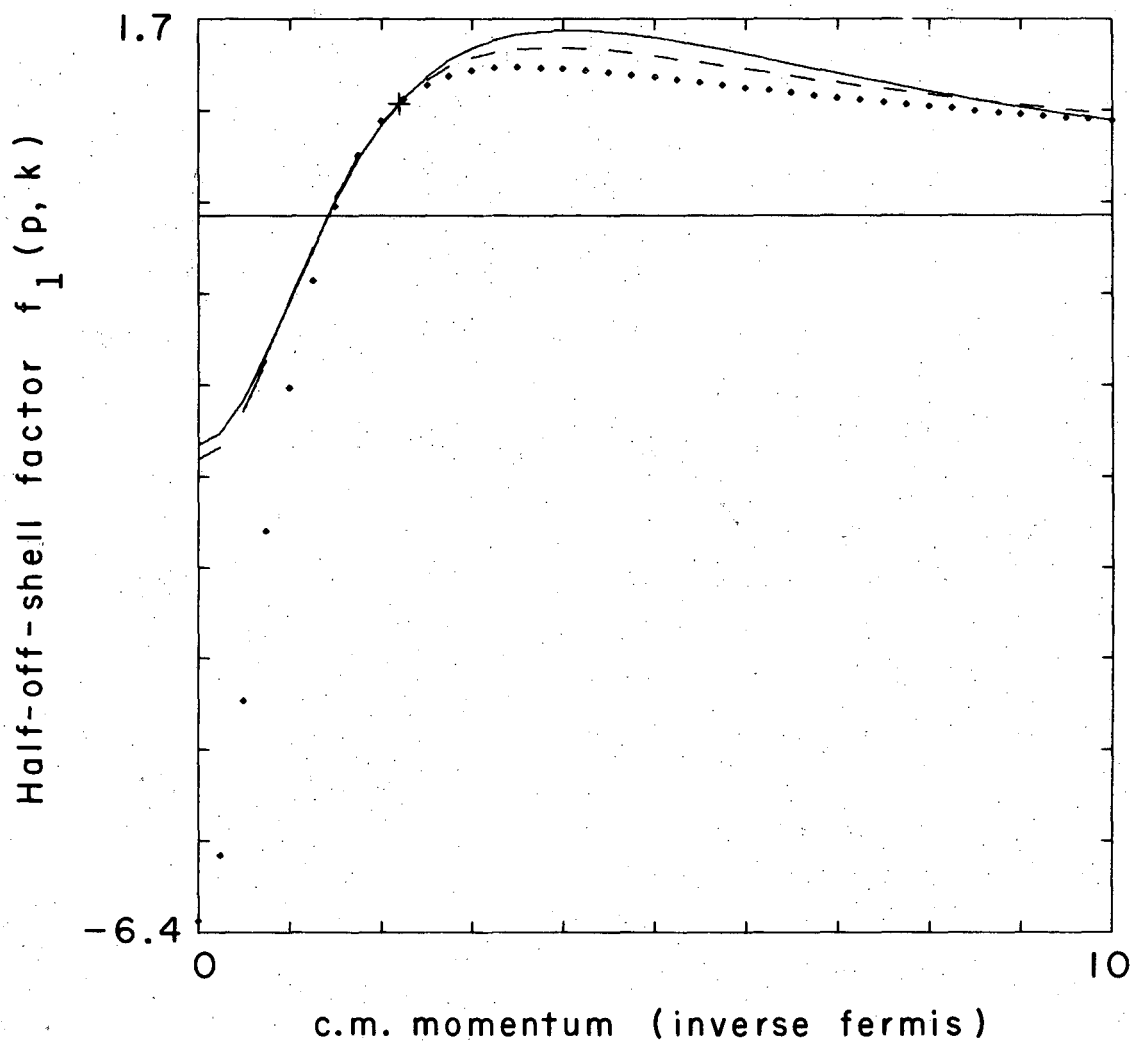

XBL6811-7215

Fig. 4

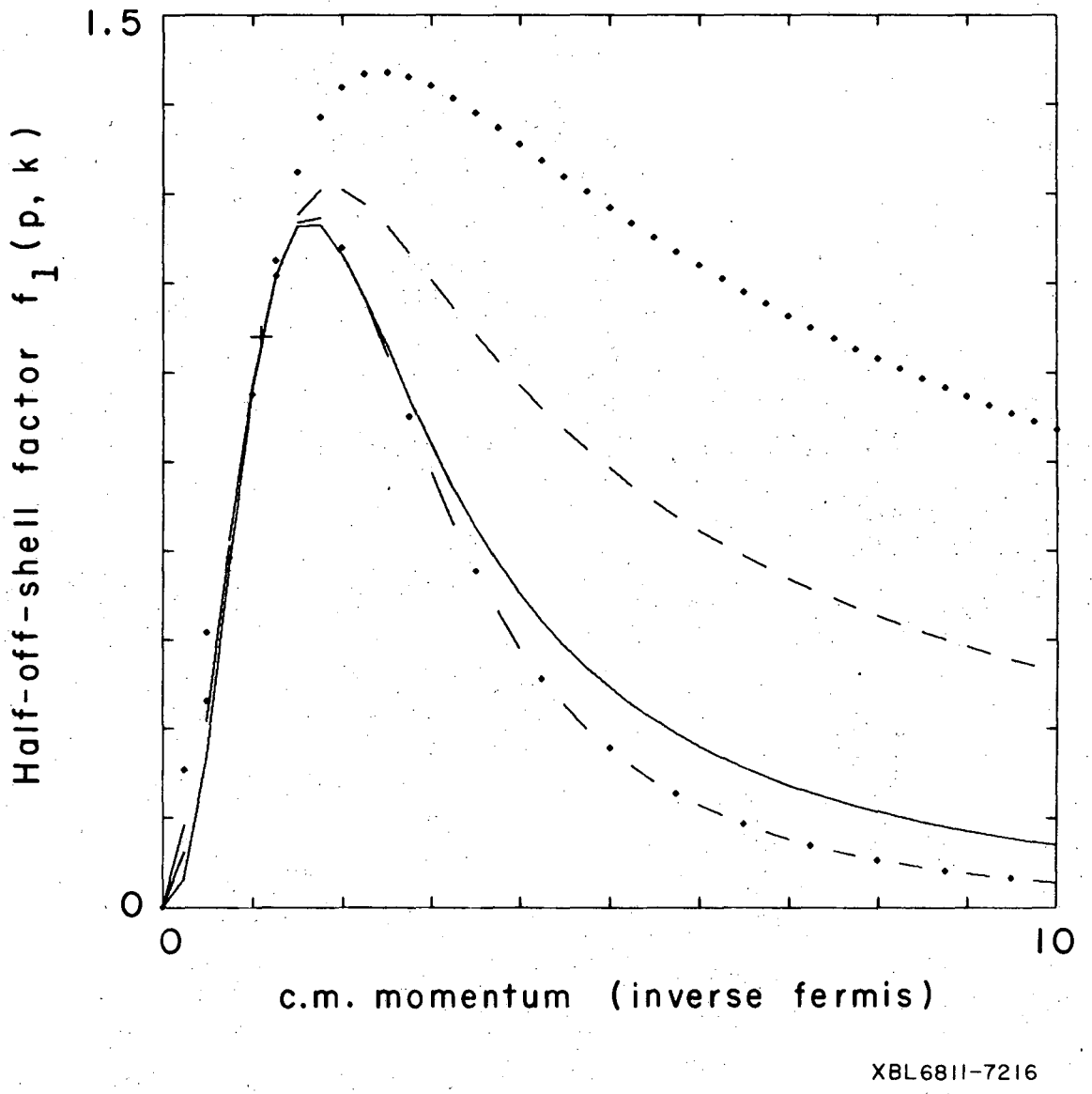
1.5
0
0
10
Half-off-shell factor $f_1(p, k)$
c.m. momentum (inverse fermis)
XBL6811-7216

Fig. 5

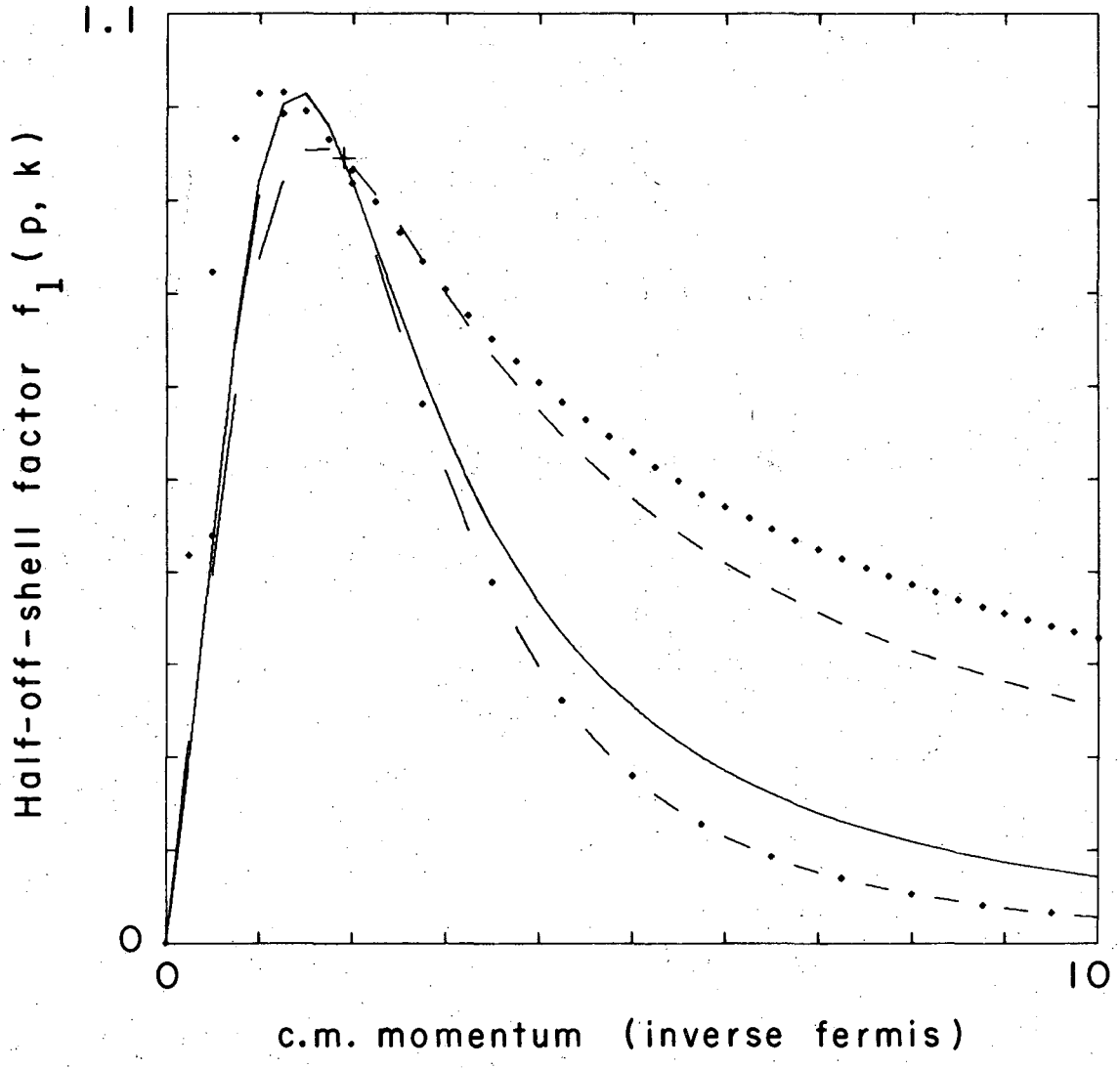

XBL6811-7217

Fig. 6

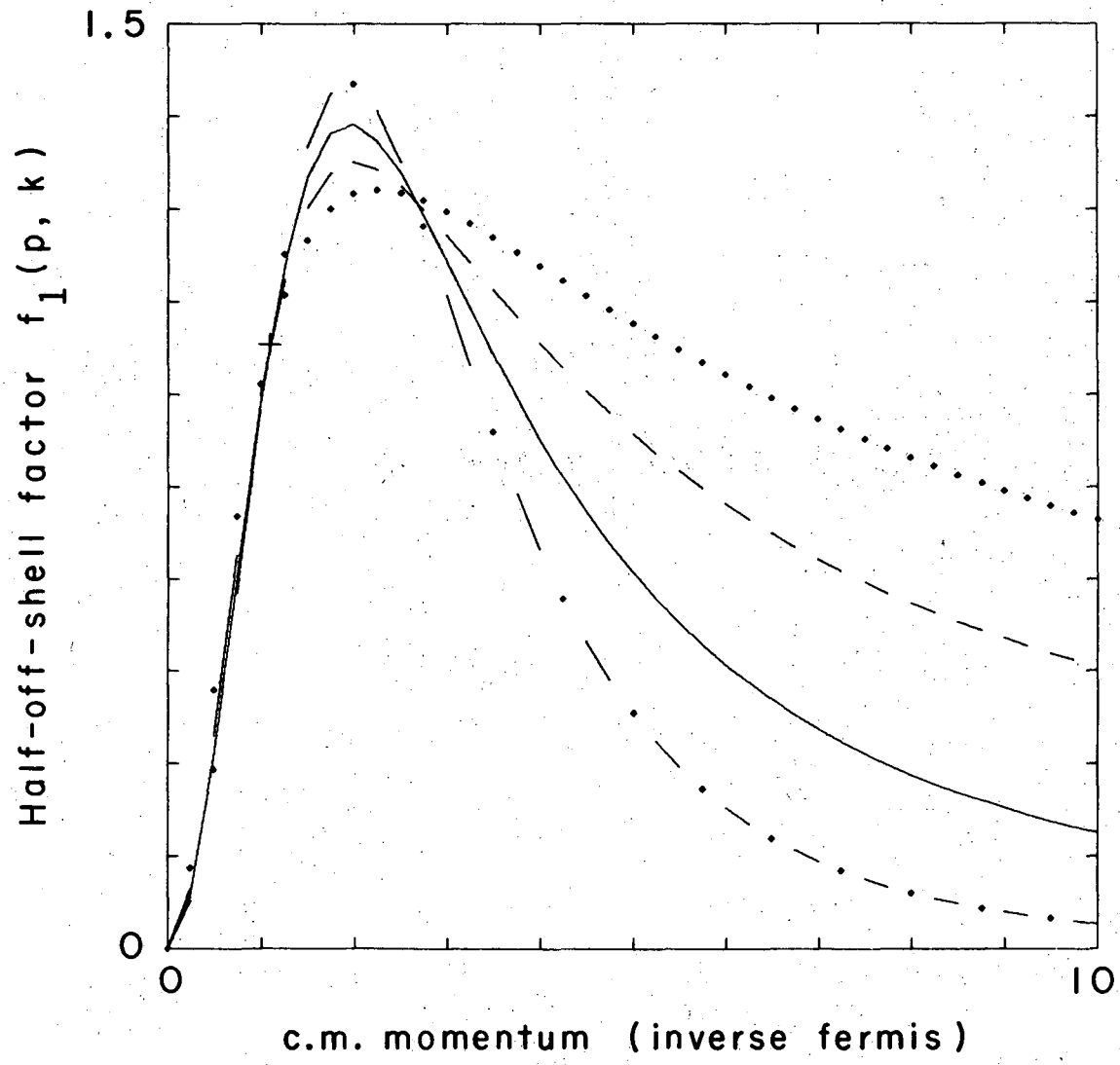

XBL6811-7218

Fig. 7

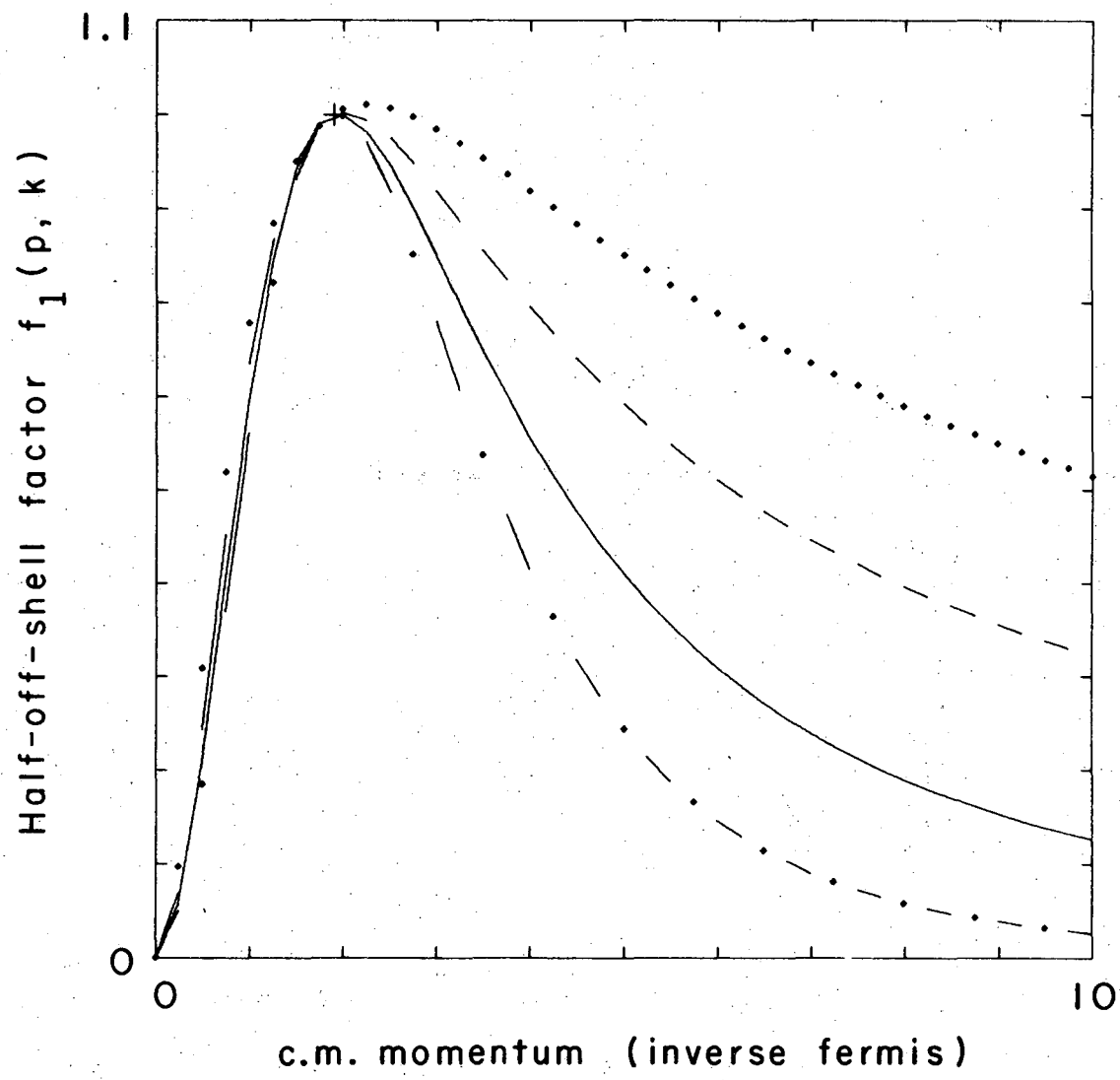

XBL6811-7219

Fig. 8

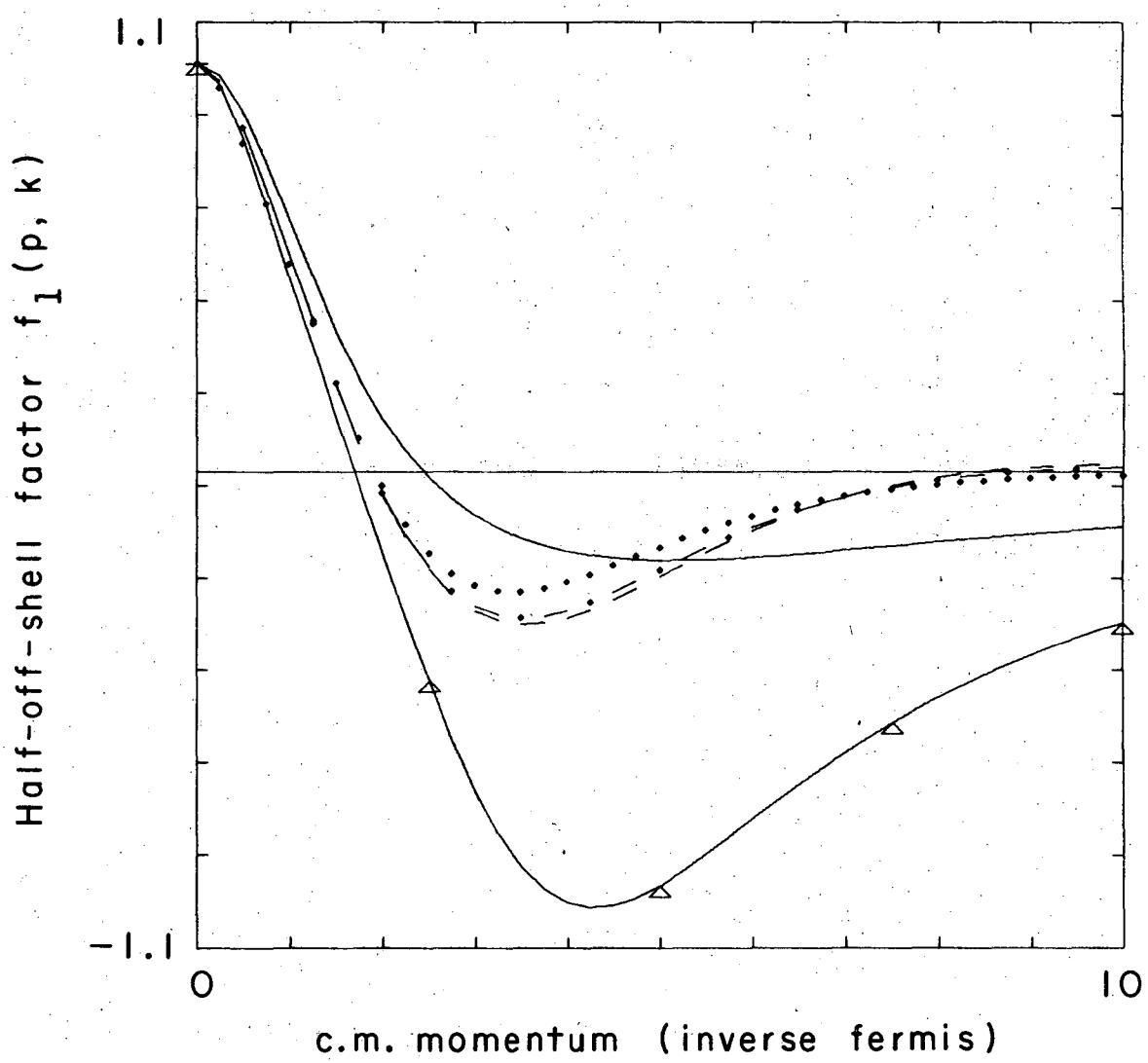

XBL6811-7220

Fig. 9

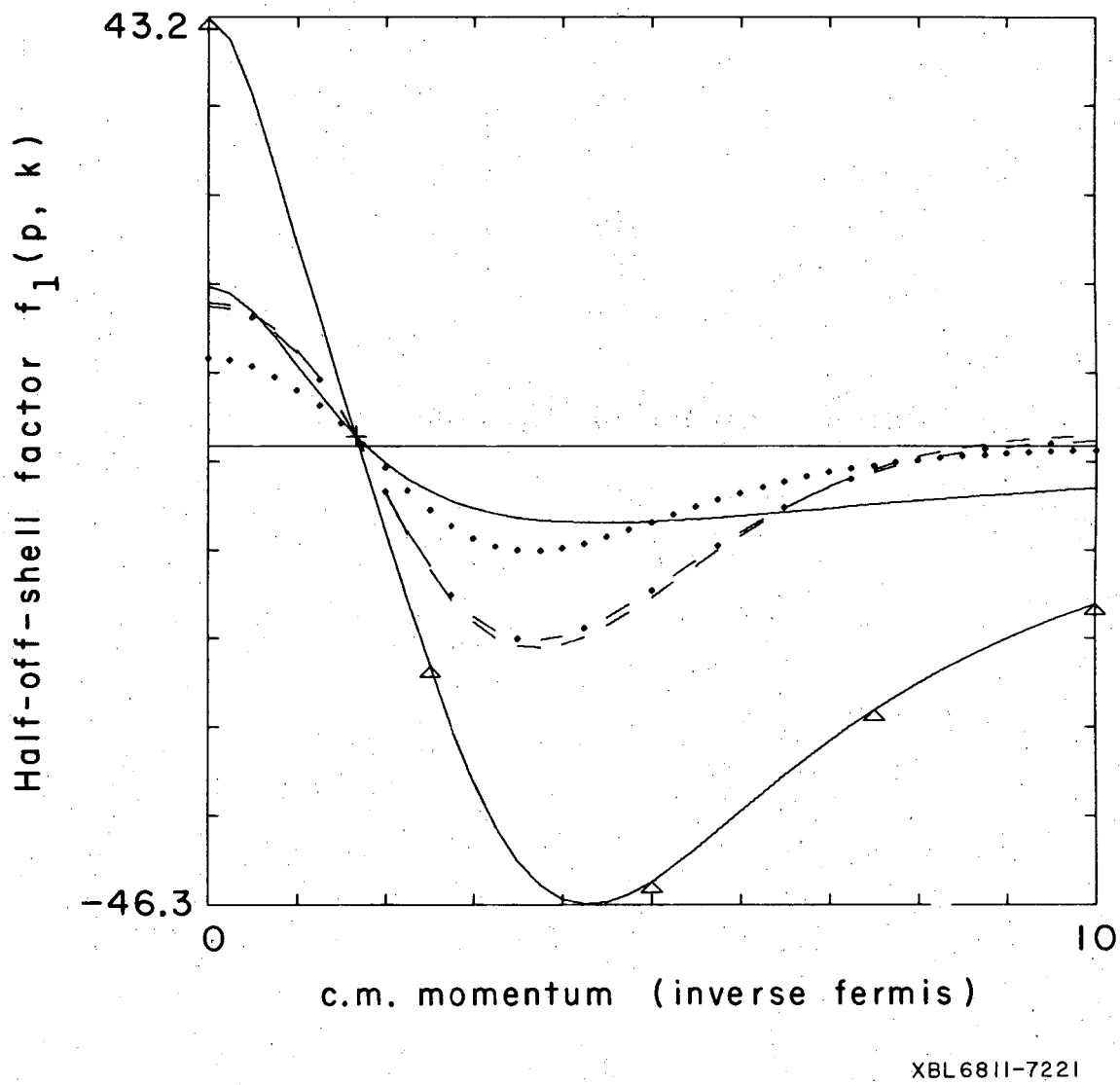
43.2
-46.3
0
10
Half-off-shell factor $f_1(p, k)$
c.m. momentum (inverse fermis)
XBL6811-7221

Fig. 10

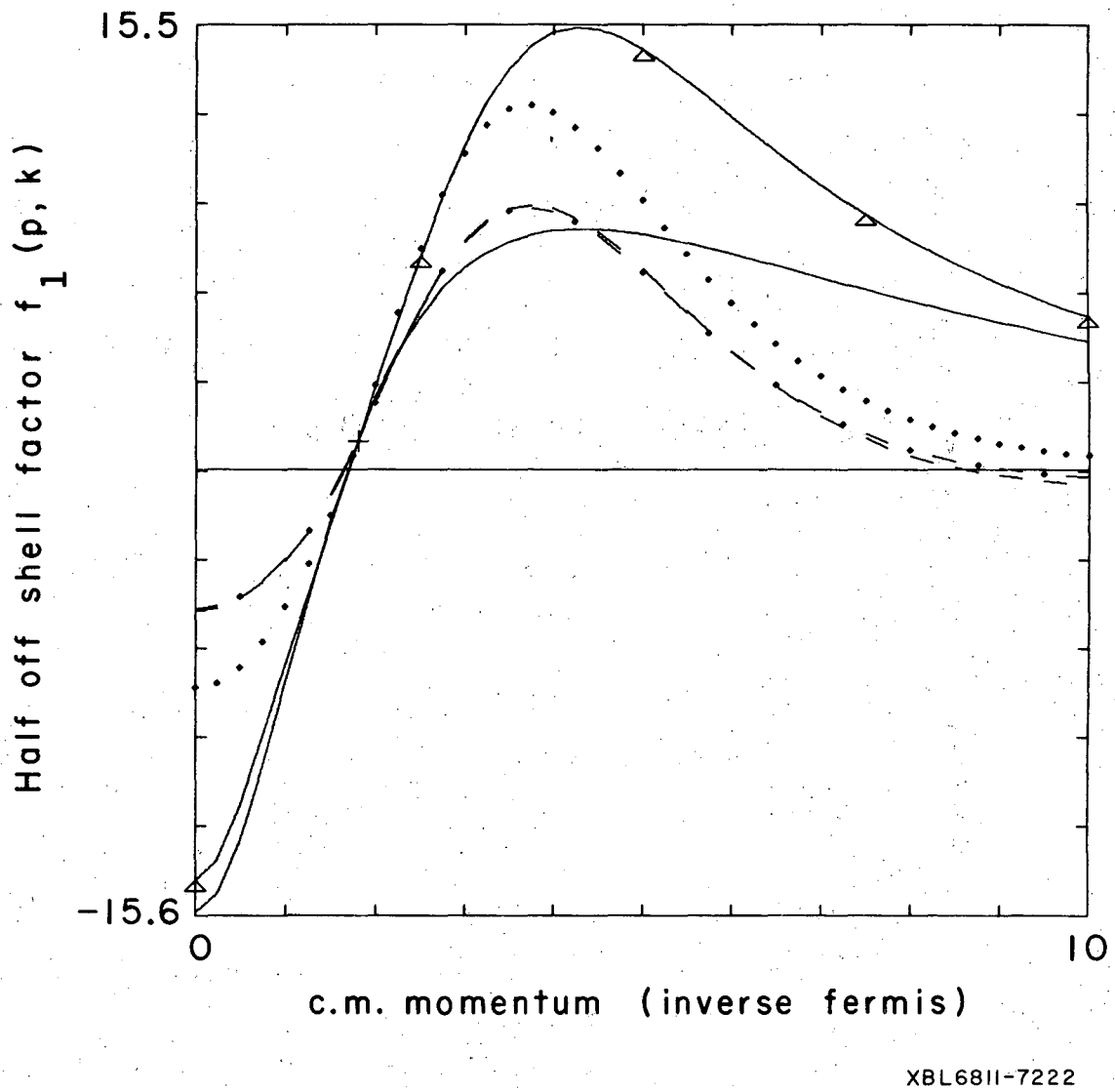
15.5
-15.6
0
10
Half off shell factor $f_1(p, k)$
c.m. momentum (inverse fermis)
XBL6811-7222

Fig. 11

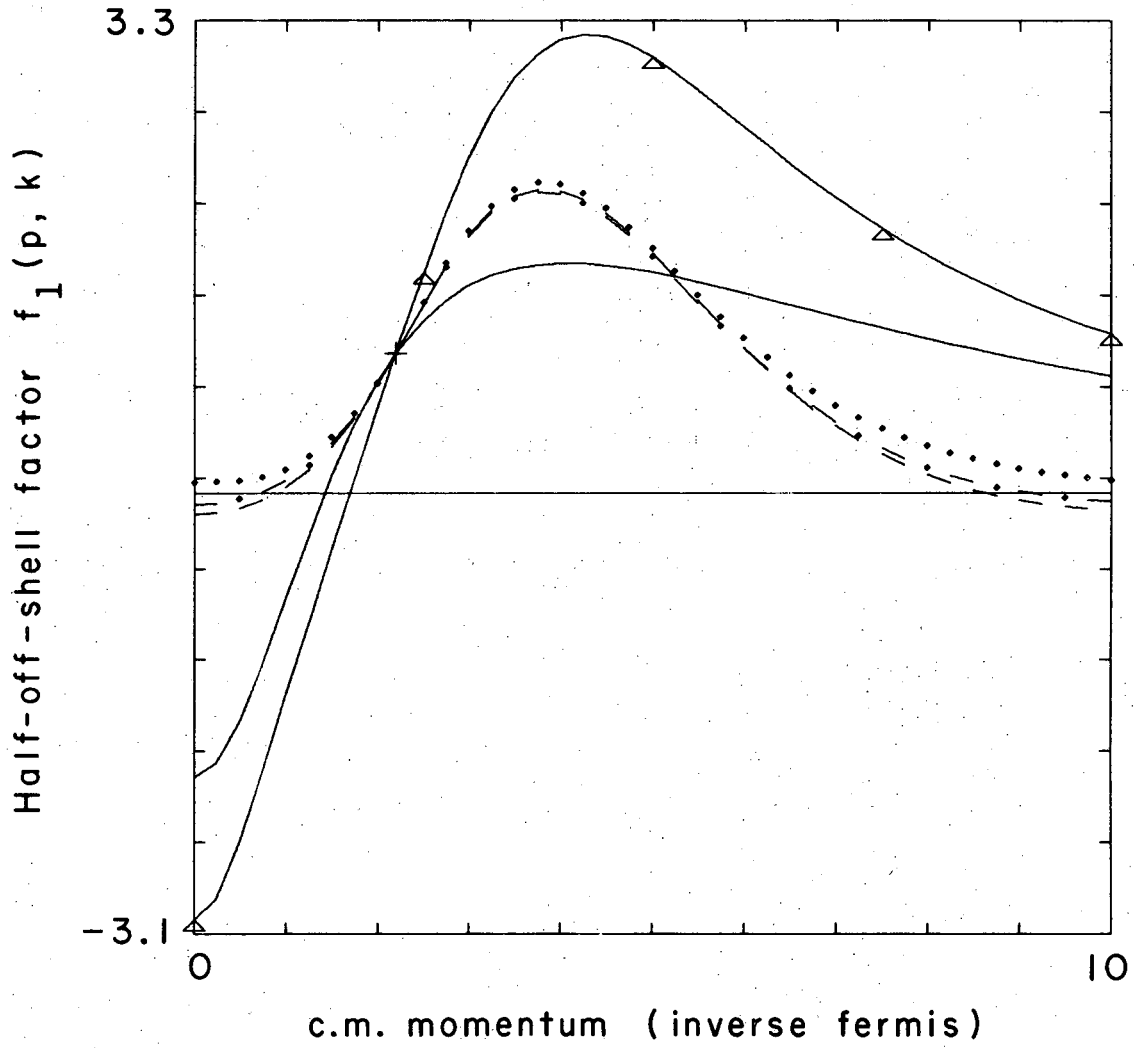

XBL6811-7223

Fig. 12

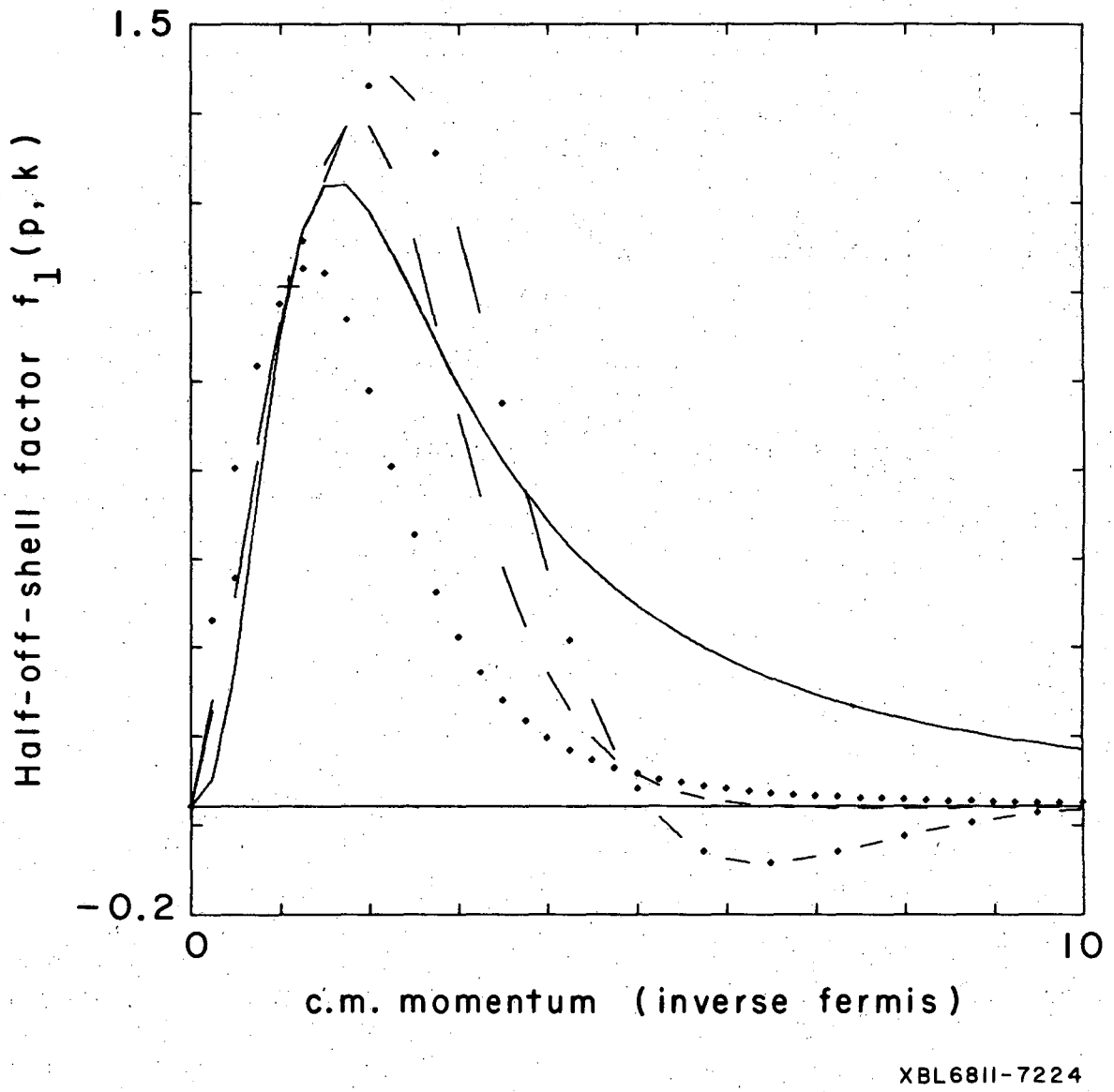
1.5
-0.2
0
10
Half-off-shell factor $f_1(p,k)$
c.m. momentum (inverse fermis)
XBL6811-7224

Fig. 13

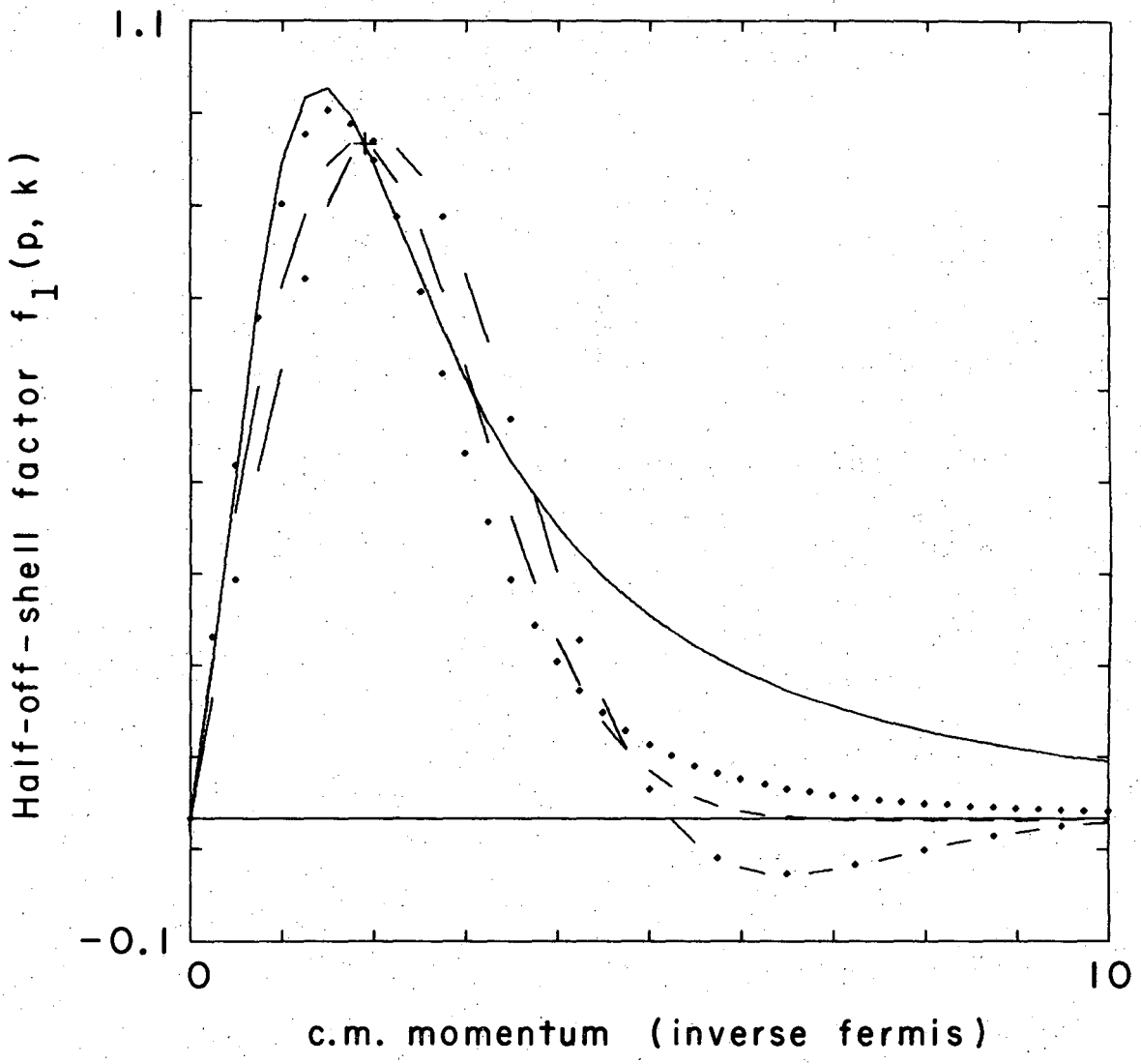

XBL6811-7225

Fig. 14

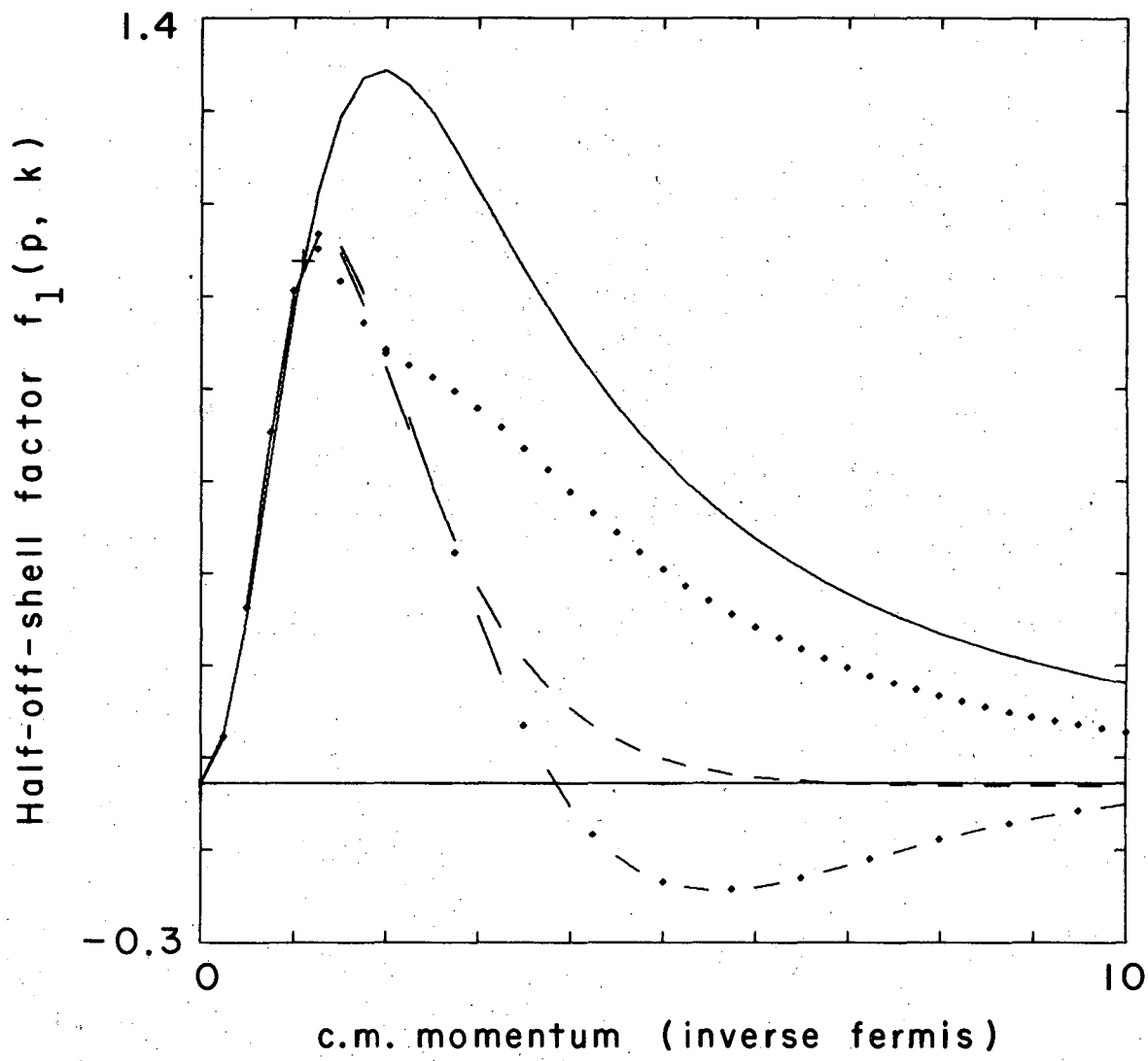

XBL6811-7226

Fig. 15

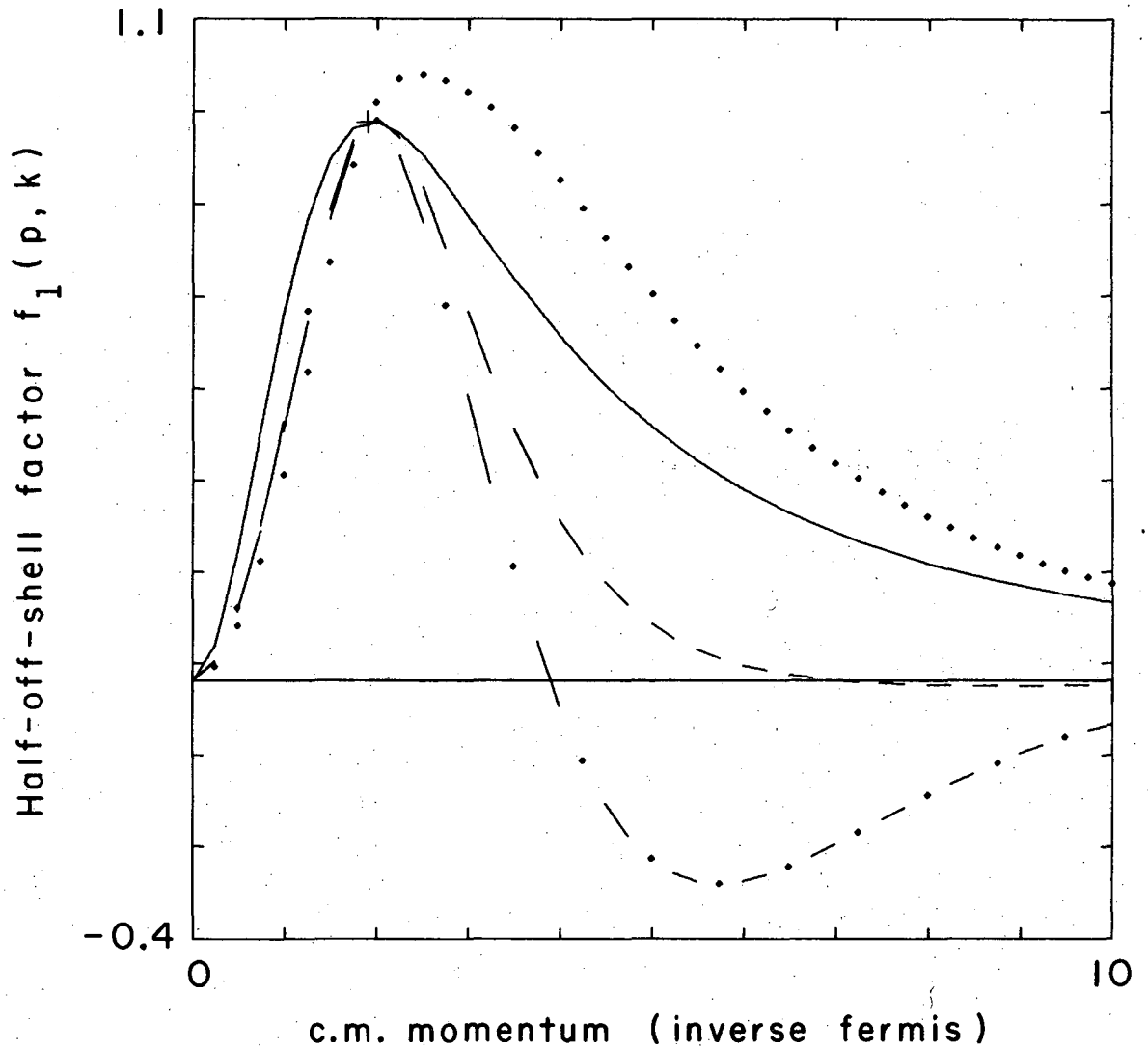

XBL6811-7227

Fig. 16

LEGAL NOTICE

This report was prepared as an account of Government sponsored work. Neither the United States, nor the Commission, nor any person acting on behalf of the Commission:

A. Makes any warranty or representation, expressed or implied, with respect to the accuracy, completeness, or usefulness of the information contained in this report, or that the use of any information, apparatus, method, or process disclosed in this report may not infringe privately owned rights; or

B. Assumes any liabilities with respect to the use of, or for damages resulting from the use of any information, apparatus, method, or process disclosed in this report.

As used in the above, "person acting on behalf of the Commission" includes any employee or contractor of the Commission, or employee of such contractor, to the extent that such employee or contractor of the Commission, or employee of such contractor prepares, disseminates, or provides access to, any information pursuant to his employment or contract with the Commission, or his employment with such contractor.

TECHNICAL INFORMATION DIVISION
LAWRENCE RADIATION LABORATORY
UNIVERSITY OF CALIFORNIA
BERKELEY, CALIFORNIA 94720